Passively Q-switched green laser operation using CdTe/CdS quantum dots

(Invited Paper)

Xigun Yan (严希滚)[1,3], Saiyu Luo (罗塞雨)[1], Bin Xu (徐 斌)[1,*], Huiying Xu (许惠英)[1], Zhiping Cai (蔡志平)[1], Jingzhou Li (李京周)[2], Hongxing Dong (董红星)[2], Long Zhang (张 龙)[2], and Zhengqian Luo (罗正钱)[1,3,]**

[1]*Department of Electronic Engineering, Xiamen University, Xiamen 361005, China*

[2]*Key Laboratory of Materials for High-Power Laser, Shanghai Institute of Optics and Fine Mechanics, Chinese Academy of Science, Shanghai 201800, China*

[3]*Shenzhen Research Institute of Xiamen University, Shenzhen 518057, China*

**Corresponding author: xubin@xmu.edu.cn; **corresponding author: zqluo@xmu.edu.cn*

Received September 22, 2017; accepted November 10, 2017; posted online December 26, 2017

The direct generation of passively Q-switched lasers at a green wavelength has rarely been investigated in the past. In this Letter, we demonstrate a passively Q-switched praseodymium-doped yttrium lithium fluoride green laser at 522 nm using CdTe/CdS quantum dots as a saturable absorber. A maximum average output power of 33.6 mW is achieved with the shortest pulse width of 840 ns. The corresponding pulse energy and peak power reached 0.18 μJ and 0.21 W, respectively. To the best of our knowledge, this is the first demonstration in regard to a quantum dots saturable absorber operating in the green spectral region.

OCIS codes: 140.3480, 140.3540, 140.3580.

doi: 10.3788/COL201816.020005.

Passive Q-switching and mode locking are two crucial technologies for short and ultrashort pulse generation. Based on these two technologies, efficient, reliable, and cost-effective saturable absorbers are always desirable. If the saturable absorber is also universal for laser operation with large wavelength range, it would be the desired candidate for researchers. Most conventional saturable absorbers, like Cr^{4+}-, V^{3+}-, Co^{2+}-, and Cr^{2+}-doped materials[1–6], as well as the well-known semiconductor saturable absorber mirror (SESAM)[7–9], cannot nicely match all these wanted merits.

During the past decade, a kind of new saturable absorber on the basis of various nanomaterials has been greatly developed. Mostly, these nanomaterial's saturable absorbers exhibit some advantages, including broadband saturable absorption, low cost, and easy fabrication. These advantages are indeed not covered for the conventional saturable absorbers. As a consequence, because of these desirable advantages, nanomaterials used for saturable absorbers have become an increasingly popular research topic, and relevant studies have involved Q-switched and mode-locked laser operation from visible to middle infrared[10–26], such as carbon nanotube[10–12] and other two-dimensional (2D) nanomaterials like graphene[13–15], topological insulators (TIs)[16–20], transition metal dichalcogenides (TMDCs)[21–27], black phosphorus[28–30], etc. Especially, at present, no conventional saturable absorbers as mentioned above, i.e., SESAM, Cr^{4+}-, V^{3+}-, Co^{2+}-, and Cr^{2+}-doped materials, have been reported to be a Q-switcher or mode locker for green laser emission. Recently, a green laser at 522 nm has been successfully Q-switched and mode-locked using MoS_2[21,22].

On the other hand, quantum dots (QDs) used as saturable absorbers have also attracted attention recently because of their relatively broadband absorption spectrum, arising from inhomogeneous broadening associated with a variation of dot sizes[31]. A main advantage of QDs over those 2D nanomaterials is that, because of high-level controllability over the size of the crystals, it is possible to have very precise control over the conductive properties of the material. The smaller the size of the crystal and the larger the band gap, the greater the difference in energy between the highest valence band and the lowest conduction band becomes. Although the energy band gap of the 2D nanomaterials can also be tuned by increasing their number of layers, the multilayer 2D nanomaterials will transform into indirect semiconductors, which will lead to a greatly reduced electron transition rate. As a result, it results in large saturable intensities for 2D nanomaterials saturable absorbers[32]. Additionally, compared to their quantum well counterparts, QDs could, in principle, offer lower saturation fluence, faster recovery time, and lower non-saturable losses[32,33]. Recently, using QDs as saturable absorber, we operated passively Q-switched visible lasers at 721, 640, and 607 nm[34].

In this work, core/shell structure QDs, CdTe/CdS, were fabricated by a liquid-phase method, which provides a much less expensive and far simpler alternative to epitaxially grown semiconductors. The core/shell materials of CdTe/CdS QDs have the same lattice structure and exhibit a small lattice mismatch, which caused the QDs to have a

good chemical stability. At the same time, the CdTe core has a larger dielectric constant, leading to a relatively stronger dielectric screening. By operating a blue diode-pumped Q-switched praseodymium-doped yttrium lithium fluoride (Pr:YLF) laser at 522 nm with the CdTe/CdS QD as a saturable absorber, we have further extended the operational wavelength of the QD to green.

The detailed fabrication process can be found in our previous publication[34]. Figure 1 shows the measured absorbance and photoluminescence (PL) curves of the QDs sample using a Shimadzu UV-2450 ultraviolet-visible (UV-vis) spectrophotometer and a Cary Eclipse (Varian) fluorescence spectrophotometer. The inset shows the sizes of the QDs measured by transmission electron microscopy (TEM, JEOL-2100). The saturable absorption property of the QDs sample was investigated using an open aperture Z-scan system with femtosecond laser pulses at 515 nm, which closely corresponds to the investigated laser oscillation at 522 nm. The pulse width of a fiber laser source was 340 fs with a repetition rate of 1 kHz. Figure 2 clearly shows that the normalized transmissions increased gradually with the approaching of the QD sample to the focus point of the open aperture Z-scan system, which indicated that the absorption of the QDs became saturated with the increase of the incident pump intensity/energy. The CdTe/CdS saturable absorber was fabricated by transferring the CdTe/CdS dispersion onto an anti-reflection coated 0.5-mm-thick BK7 glass thin plate via a spin coating method. Measuring the small signal transmission of the CdTe/CdS saturable absorber using a PerkinElmer Lambda 750 Spectrometer gave a transmission of about 89.3% at 522 nm, which indicates that the linear loss of the CdTe/CdS thin film is about 10.7%.

The experimental setup is schematically shown in Fig. 3. The pump source is an InGaN diode laser emitting at about 444 nm of peak wavelength with maximum output power of about 1.8 W. The pump beam was injected into

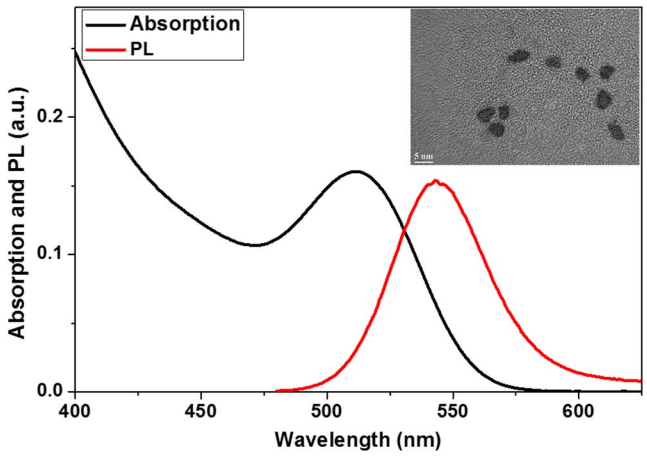

Fig. 1. (Color online) Absorbance and PL curves of the green colloidal quantum dot (CQD) sample with an inset of the TEM image.

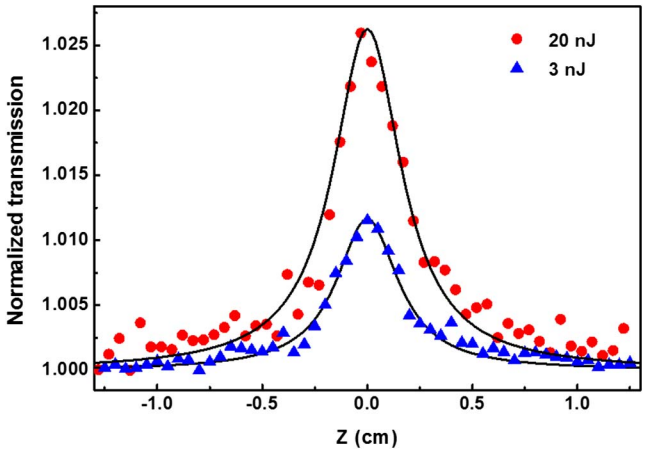

Fig. 2. (Color online) Open aperture Z-scan measurements of the saturable absorption property of the as-fabricated CQD, using a femtosecond laser source at 515 nm.

the laser crystal by a plane-convex aspherical focusing lens with focal length of 50 mm. The laser resonator consisted of a compact two-mirror near hemispherical configuration with a resonator length of about 47 mm. The flat input mirror (IM) has a high transmission of about 90% at the pumping wavelength, high reflection of more than 99.9% at 522 nm, and high transmissions of about 34% at 607 nm and 89% at 639 nm. The coating of the IM simultaneously ensures an effective pump injection and mode suppressions of those high-gain lines at orange and red. The output coupler (OC) with a curvature radius of 50 mm has a transmission of about 1.9% at 522 nm.

The gain medium was a 0.2 at% -doped Pr:YLF crystal with a cross section of 2 mm × 2 mm and a length of 8 mm. The ratio of single pass absorption was measured to be about 90% of the maximum pump power. The laser crystal was mounted inside a copper block and was wrapped with indium foil to strengthen the thermal contact between the copper block and laser crystal. The copper block was connected to a chiller with the temperature set at 16°C. During Q-switching, the CdTe/CdS QDs saturable absorber was inserted into the laser resonator.

Green laser emission at 522 nm was first demonstrated in the continuous-wave regime, and Fig. 4 shows the dependence of output power on absorbed power. A maximum output power up to 262 mW was achieved, and the slope efficiency with respect to absorbed power was

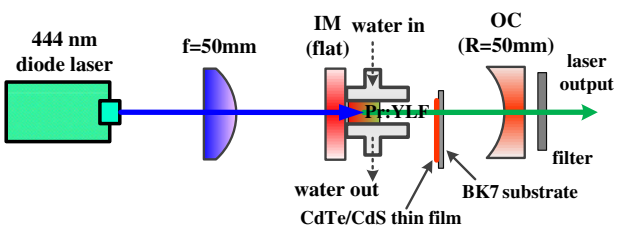

Fig. 3. Schematic of blue diode-pumped passively Q-switched Pr:YLF laser at 522 nm.

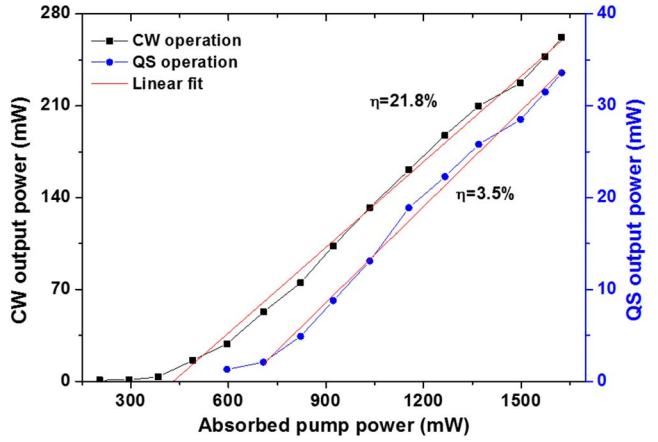

Fig. 4. (Color online) Green laser output power characteristics in continuous-wave and Q-switching regimes.

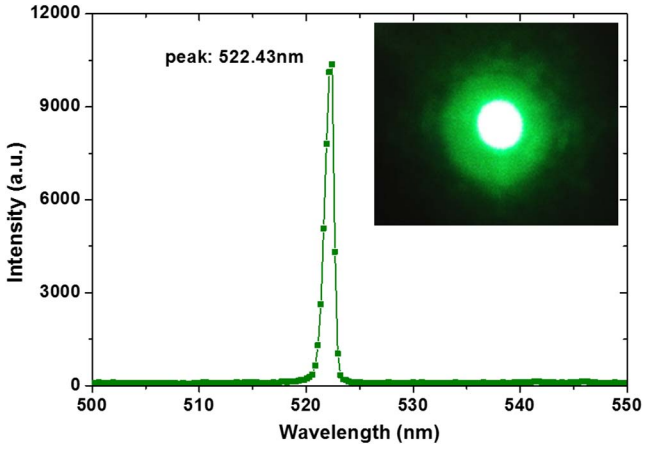

Fig. 5. Spectrum of the Q-switched Pr:YLF laser at 522 nm. Inset: photograph of the green laser beam spot.

linearly fitted to be about 21.8%. By optimizing the dopant concentration and length of the Pr:YLF crystal, the transmission of the OC, as well as the overlap efficiency between the pump beam and cavity mode and far better laser performance, could be realized. However, the main purpose of this work is not to achieve a high-power continuous-wave laser, and the present result was obtained by using the available experimental components.

After inserting the as-prepared CdTe/CdS QDs saturable absorber into the laser resonator, Q-switched laser pulse trains can be observed at 595 mW of absorbed power, and the maximum average output power reached 33.6 mW, thus leading to a slope efficiency of about 3.5%, as shown in Fig. 4. Compared with the continuous-wave laser performance, the present Q-switched laser has showed degraded performance with higher threshold, far lower average output power, and slope efficiency, which should be ascribed to the insertion loss and Fresnel reflection loss of the glass substrate, as well as the transfer quality of the CdTe/CdS QDs. All these aspects should be improved in the near future for better laser performance of a Q-switched Pr:YLF green laser. The laser spectrum of the Q-switched operation was shown in Fig. 5, indicating a peak wavelength at 522.43 nm. The inset in Fig. 5 shows the green laser beam spot.

Figures 6(a) and 6(b) show the typical pulse trains, respectively, with pulse repetition rates of 79.6 kHz at 4.9 mW and 168.9 kHz at about 28.5 mW. When the average output power reached about 28.5 mW, we obtained the narrowest pulse width with a time duration of about 840 ns, as shown in Fig. 7. To reduce the time duration of the present pulsed laser, a saturable absorber with a larger modulation depth and using a short laser resonator could work. This is why a Q-switched microchip laser could be operated to reach a pulse width to the scale of picoseconds[35].

We further plotted the entire variations of the pulse width together with the pulse repetition rate with the increase of absorbed power in Fig. 8. It clearly shows that the pulse width decreased fast at first by increasing the

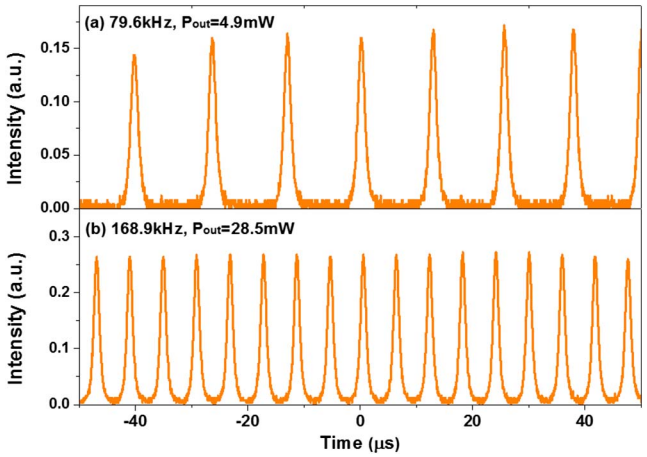

Fig. 6. Pulse trains measured at average output powers of (a) 4.9 mW at the threshold with a repetition rate of 79.6 kHz and (b) 28.5 mW with a repetition rate of 168.9 kHz.

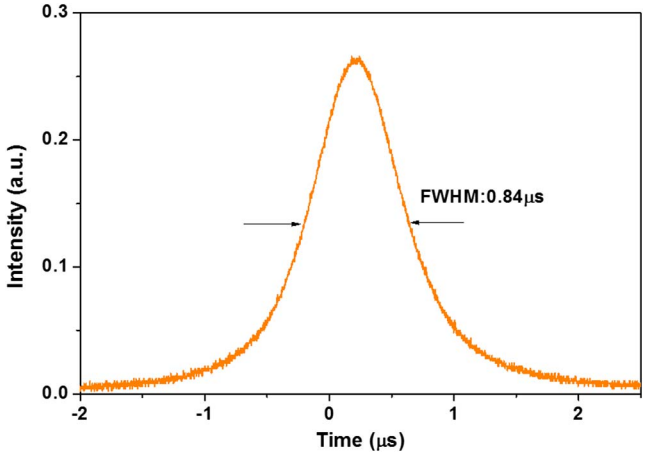

Fig. 7. Narrowest pulse with time duration of about 0.84 μs.

absorbed power to about 1000 mW. Further increasing the absorbed power to about 1500 mW, the pulse width narrowed with a weak tendency. In fact, the pulse width

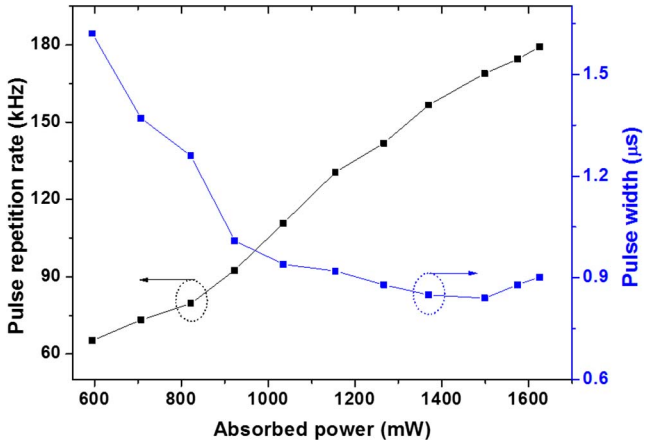

Fig. 8. (Color online) Variations of pulse widths and pulse repetition rates with the increase of absorbed pump powers for a 522 nm Q-switched Pr:YLF laser.

showed saturation at about 1500 mW with the shortest time duration of about 840 ns, as above mentioned. Afterward, the pulse width augmented to about 0.9 μs at an achievable maximum absorbed power of 1.62 W. Such Q-switching pulse broadening can still be basically explained by the small modulation depth of the saturable absorber, thus leading to the bleaching of it due to the high intracavity intensity. At the same time, such bleaching could also destabilize the Q-switching operation. In Fig. 8, the pulse repetition rate curve shows a monotonous increase from 65.2 to 179.3 kHz with the increase of the absorbed power; although, a weak saturation tendency can be observed.

With these pulse parameters data, we estimated two other important pulse parameters, i.e., single pulse energy and pulse peak power, as shown in Fig. 9. The maximum pulse energy is about 0.18 μJ, and the corresponding pulse peak power is about 0.21 W. Moreover, with the increase of the absorbed power, saturation phenomena for the pulse parameters were also observed, especially for pulse peak power because of the rollover of the pulse width at high pump power. Zhang *et al.*[21] reported continuous-wave and MoS_2-based passive Q-switched Pr:GLF lasers at 522 nm. For continuous-wave operation, the authors achieved a maximum output power of 178 mW, while, for passive Q-switching, the pulse parameter values are 10 mW of the maximum average output power, 579 ns of pulse width, 154 mW of peak power, and 101 nJ of pulse energy. Therefore, our present results indicate better laser performances under the continuous-wave and Q-switching regimes.

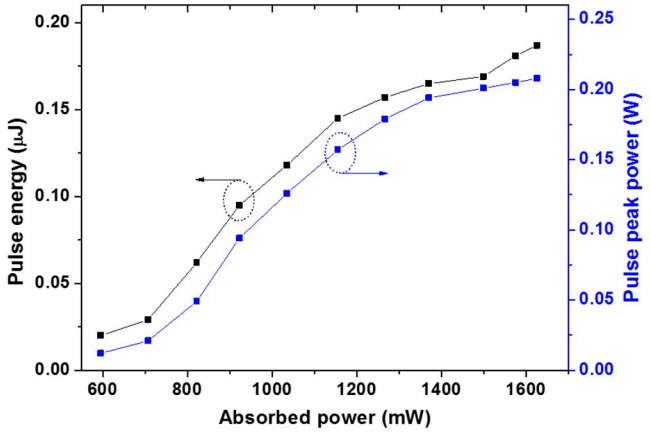

Fig. 9. (Color online) Corresponding dependence of pulse energy and pulse peak power on absorbed pump power.

In conclusion, using a Pr:YLF crystal as the gain medium, we operate a continuous-wave laser at 522 nm with maximum output power of 262 mW and slope efficiency of about 21.8%. Using CdTe/CdS QDs as a saturable absorber, passive Q-switching is also investigated with maximum average output power of 33.6 mW and the shortest pulse width of 840 ns. The corresponding pulse energy and peak power reach 0.18 μJ and 0.21 W, respectively. Further scaling the performance of the passive Q-switched green laser to a shorter pulse width and larger pulse energy and peak power could resort to fabricating the CdTe/CdS QDs saturable absorber with a large modulation depth.

This work was supported by the National Natural Science Foundation of China (No. 61575164), the Natural Science Foundation of Fujian Province of China (Nos. 2017J06016 and 2014J01251), and the Shenzhen Science and Technology Projects (No. JCYJ20160414160109018).

References

1. K. Spariosu, W. Chen, R. Stultz, M. Birnbaum, and A. V. Shestakov, Opt. Lett. **18**, 814 (1993).
2. A. Agnesi, A. Guandalini, G. Reali, J. K. Jabczynski, K. Kopczynski, and Z. Mierczyk, Opt. Commun. **194**, 429 (2001).
3. A. V. Podlipensky, V. G. Shcherbitsky, N. V. Kuleshov, V. P. Mikhailov, V. I. Levchenko, and V. N. Yakimovich, Opt. Lett. **24**, 960 (1999).
4. E. C. Ji, M. M. Nie, X. Fu, Z. G. Guan, and Q. Liu, Opt. Lett. **42**, 2555 (2017).
5. J. L. Lan, Z. Y. Zhou, X. F. Guan, B. Xu, H. Y. Xu, Z. P. Cai, X. D. Xu, D. Z. Li, and J. Xu, Opt. Mater. Express **7**, 1725 (2017).
6. F. Canbaz, I. Yorulmaz, and A. Sennaroglu, Opt. Lett. **42**, 1656 (2017).
7. J. A. Au, S. F. Schaer, R. Paschotta, C. Honninger, U. Keller, and M. Moser, Opt. Lett. **24**, 1281 (1999).
8. C. R. Phillips, A. S. Mayer, A. Klenner, and U. Keller, Opt. Express **22**, 6060 (2014).
9. L. C. Kong, Z. P. Qin, G. Q. Xie, X. D. Xu, J. Xu, P. Yuan, and L. J. Qian, Opt. Lett. **40**, 356 (2015).
10. J. L. Lan, Z. Y. Zhou, X. F. Guan, B. Xu, H. Y. Xu, and Z. P. Cai, J. Opt. **19**, 045504 (2017).
11. S. M. Azooz, F. Ahmad, H. Ahmad, S. W. Harun, B. A. Hamida, S. Khan, A. Halder, M. C. Paul, M. Pal, and S. K. Bhadra, Chin. Opt. Lett. **13**, 030602 (2015).
12. D. V. Khudyakov, A. S. Lobach, and V. A. Nadtochenko, Opt. Lett. **35**, 2675 (2010).
13. H. Zhang, D. Y. Tang, L. M. Zhao, Q. L. Bao, and K. P. Loh, Opt. Express **17**, 17630 (2009).

14. B. Xu, Y. Wang, Y. J. Cheng, H. Yang, H. Y. Xu, and Z. P. Cai, J. Opt. **17**, 105501 (2015).
15. C. Zuo, J. Hou, B. Zhang, and J. He, Chin. Opt. Lett. **13**, 021401 (2015).
16. Z. Luo, C. Liu, Y. Huang, D. Wu, J. Wu, H. Xu, Z. Cai, Z. Lin, L. Sun, and J. Weng, IEEE J. Sel. Top. Quantum Electron. **20**, 0902708 (2014).
17. Z. C. Luo, M. Liu, H. Liu, X. W. Zheng, A. P. Luo, C. J. Zhao, H. Zhang, S. C. Wen, and W. C. Xu, Opt. Lett. **38**, 5212 (2013).
18. B. Xu, Y. Wang, J. Peng, Z. Q. Luo, H. Y. Xu, Z. P. Cai, and J. Weng, Opt. Express **23**, 7674 (2015).
19. P. H. Tang, X. Q. Zhang, C. J. Zhao, Y. Wang, H. Zhang, D. Y. Shen, S. C. Wen, D. Y. Tang, and D. Y. Fan, IEEE Photon. J. **5**, 1500707 (2013).
20. C. J. Zhao, H. Zhang, X. Qi, Y. Chen, Z. T. Wang, S. C. Wen, and D. Y. Tang, Appl. Phys. Lett. **101**, 211106 (2012).
21. Y. X. Zhang, S. X. Wang, D. Wang, H. H. Yu, H. J. Zhang, Y. X. Chen, L. M. Mei, A. D. Lieto, M. Tonelli, and J. Y. Wang, IEEE Photon. Tech. Lett. **28**, 197 (2016).
22. Y. X. Zhang, H. H. Yu, R. Zhang, G. Zhao, H. J. Zhang, Y. X. Chen, L. M. Mei, M. Tonelli, and J. Y. Wang, Opt. Lett. **42**, 547 (2017).
23. H. Zhang, S. B. Lu, J. Zheng, J. Du, S. C. Wen, D. Y. Tang, and K. P. Loh, Opt. Express **22**, 7249 (2014).
24. B. Xu, Y. J. Cheng, Y. Wang, Y. Z. Huang, J. Peng, Z. Q. Luo, H. Y. Xu, Z. P. Cai, J. Weng, and R. Moncorgé, Opt. Express **22**, 28934 (2014).
25. K. Wu, X. Y. Zhang, J. Wang, X. Li, and J. P. Chen, Opt. Express **23**, 11453 (2015).
26. Z. Q. Luo, D. D. Wu, B. Xu, H. Y. Xu, Z. P. Cai, J. Peng, J. Weng, S. Xu, C. H. Zhu, F. Q. Wang, Z. P. Sun, and H. Zhang, Nanoscale **8**, 1066 (2016).
27. Y. Huang, Z. Luo, Y. Li, M. Zhong, B. Xu, K. Che, H. Xu, Z. Cai, J. Peng, and J. Weng, Opt. Express **22**, 25258 (2014).
28. Y. Chen, G. B. Jiang, S. Q. Chen, Z. N. Guo, X. F. Yu, C. J. Zhao, H. Zhang, Q. L. Bao, S. C. Wen, D. Y. Tang, and D. Y. Fan, Opt. Express **23**, 12823 (2015).
29. Z. C. Luo, M. Liu, Z. N. Guo, X. F. Jiang, A. P. Luo, C. J. Zhao, X. F. Yu, W. C. Xu, and H. Zhang, Opt. Express **23**, 20030 (2015).
30. L. C. Kong, Z. P. Qin, G. Q. Xie, Z. N. Guo, H. Zhang, P. Yuan, and L. J. Qian, Laser Phys. Lett. **13**, 045801 (2016).
31. A. A. Lagatsky, C. G. Leburn, C. T. A. Brown, W. Sibbett, S. A. Zolotovskaya, and E. U. Rafailov, Prog. Quantum Electron. **34**, 1 (2010).
32. J. Z. Li, S. F. Zhang, H. X. Dong, Y. F. Ma, B. Xu, J. Wang, Z. P. Cai, Z. H. Chen, and L. Zhang, Part. Part. Syst. Charact. **34**, 1600193 (2017).
33. V. G. Savitski, P. J. Schlosser, J. E. Hastie, A. B. Krysa, J. S. Roberts, M. D. Dawson, D. Burns, and S. Calvez, IEEE Photon. Tech. Lett. **22**, 209 (2010).
34. B. Xu, S. Y. Luo, X. G. Yan, J. Z. Li, J. L. Lan, Z. Q. Luo, H. Y. Xu, Z. P. Cai, H. X. Dong, J. Wang, and L. Zhang, IEEE J. Sel. Top. Quantum Electron. **23**, 1900507 (2017).
35. B. Braun, F. X. Kartner, G. Zhang, M. Moser, and U. Keller, Opt. Lett. **22**, 381 (1997).